Atomic displacements on stepped (16,1,1) copper structures: A channeling study

J. C. Boulliard, C. Cohen, J. L. Domange, A. V. Drigo,* A. L'Hoir, J. Moulin, and M. Sotto
Groupe de Physique des Solides de l'Ecole Normale Supérieure, Université de Paris VII, Tour 23, 2 place Jussieu, F-75005 Paris, France

(Received 19 December 1983; revised manuscript received 5 March 1984)

By taking advantage of the channeling phenomenon in solids, stepped structures are particularly well suited for studying surface atomic displacements. In particular 90° double-alignment experiments, in which the blocking of the backscattered particles by axes of the terrace plane is studied, provide exclusive information on the first atomic plane, without any bulk contribution. Surface thermal vibrations and disorder can be studied in this way. Moreover, in these experiments, the specific relaxation of the step-edge atoms can be measured. Channeling experiments in a more standard geometry can also be performed as on flat surfaces in order to extract information on the relaxation of the whole terrace. The (16,1,1) stepped, kinkless copper structure has been studied. The main results obtained for a clean surface are the following: (1) The coherent relaxation of the surface plane is very small (at the limit of our experimental precision); however, the best fit of our results corresponds to a contraction of 3×10^{-2} Å. (2) A coherent relaxation, perpendicular to the terraces, specific to the ledge atoms, has not been detected and is hence certainly smaller than 5×10^{-2} Å. (3) There is evidence for small, quasi-isotropic, static displacements of the surface atoms, all over the surface plane of concern. These displacements, with a mean value around 0.1 Å at 300 K, are somewhat correlated and are seen in channeling in the same way as thermal vibrations, but they have a stronger temperature dependence. This type of defect is perhaps related to the stepped structure. However, since it can only be detected unambiguously in 90° double-alignment backscattering experiments, which require a stepped surface, it may well be present but unobserved in simpler structures. We have also studied the effect of oxygen coverage. The saturation coverage Θ_s has been determined quantitatively by nuclear microanalysis; it corresponds to $\Theta_s=0.5$ of a monolayer. In this case low-energy electron-diffraction patterns show the existence of surface reconstruction and faceting. The channeling results are consistent with a change from the 3×10^{-2} Å contraction observed on the clean surface to a 3×10^{-2} Å dilatation. However, they mainly point to an increase of surface disorder. The very high sensitivity of the channeling technique in the 90°-backscattering double-alignment geometry for studying surface defects and surface thermal vibrations is also discussed.

I. INTRODUCTION

In the past few years, an increasing number of channeling studies with light ions in the 100-keV to 2-MeV energy domain have been devoted to problems related to surface crystallography. This technique is particularly useful for the study of atomic displacements with respect to regular lattice sites. It appears therefore to be complementary to low-energy electron diffraction (LEED) measurements, which give information mainly related to crystallographic symmetries and for which rather extensive calculations and strong assumptions are required to evaluate the static (defects) or dynamic (thermal vibrations) atomic displacements. The major advantage of the channeling technique is that rather simple Monte Carlo simulations can be performed and compared to experimental results. In these calculations a description of the crystal (mean atomic positions and thermal vibrations) is proposed, and the only physical value required to simulate a channeling experiment in this crystal is the interatomic potential between the incoming ion and a crystal atom. Since this potential is known with high precision, a comparison between the simulations and experimental results is a good check on the crystal description assumed. However, interpretation problems clearly arise, at least for somewhat complex surface structure. For instance, it is difficult to obtain detailed information when the mean atomic static displacements of all the surface atoms are not identical [as for the (7×7) surface structure of silicon]. Even if this is not the case, a check of the crystal surface structure may still require comparison between simulation and experiment for various incident-beam directions, beam energies, crystal temperatures, etc. The problem that exists when such studies are undertaken is that the surface-peak integral measured in a channeling spectrum is in many cases due to the contribution of an average number of planes significantly larger than one. The specific contribution of the very first surface plane, which is the main one under study, is therefore not predominant. Valuable information is only reached in a limited number of favorable situations; for example, the measurements of coherent relaxations of the whole surface plane give very precise results.

Quite surprisingly, no channeling studies were ever reported on stepped surfaces. Such surfaces have been extensively studied in surface physics during the last decade[1] with a great variety of techniques. Vicinal surfaces, i.e.,

those with an orientation close to a low-index plane, provide in a natural way atomic steps of known direction and density. The existence of stable, regular steps, with terraces of quasi-identical width has been evidenced by field-ion microscopy, LEED, and electron microscopy. A great variety of fundamental surface problems is related to the existence of such surfaces: stability; influence of adsorbed species which may lead to faceting; atomic, molecular, or vacancy diffusion along the terraces; preferential adsorption sites along the step edges and relation with catalysis; atomic displacements all over the terraces induced by interactions between step edge; possible specific relaxation and enhanced thermal vibrations of the loosely bound step atoms, etc.

We shall demonstrate in this paper that channeling is particularly well adapted to study most of the structural problems listed above. Moreover, we shall also show that stepped structures make possible channeling experiments in which specific information about the first atomic plane may be obtained without any (background) bulk contribution. We thus have an ideal situation for the study of the crystallographic structure of this plane, surface thermal-vibration amplitudes, and also, perhaps, correlated vibrations.

The present work is devoted to the study of (16,1,1) stepped copper surfaces via channeling. The terraces are of (100) orientation and, in addition to specific experiments related to the study of the stepped structure which constitute the main part of the work, we have also searched for the coherent relaxation of the first atomic plane with "standard" channeling experiments. The (16,1,1) structure has been shown to be unstable when oxygen adsorption takes place.[2] This adsorption leads to faceting with the appearance of (410) and (100) domains. We have studied the influence of this process on the surface order and surface relaxation. The oxygen coverage at saturation has also been determined by nuclear microanalysis.

In all our experiments the sample was characterized by LEED and Auger spectroscopy. The experimental setup is described in Sec. II. Sample preparation and characterization are presented in Sec. III. The description of the various channeling experiments performed and their aim are given in Sec. IV. Section V presents our Monte Carlo simulatations and a discussion of the sensitivity to atomic displacements as predicted by these simulations. The experimental results are presented, discussed, and interpreted in Sec. VI.

II. APPARATUS

A. Ultrahigh-vacuum chamber and equipment

The ultrahigh-vacuum (UHV) chamber schematically represented in Fig. 1 was specially designed by us for the type of surface studies presented here and built by RIBER. It consists of a stainless-steel cylinder equipped with a 70-l/s turbomolecular pump, a 400-l/s ionic pump, and a liquid-nitrogen trap operating with a titanium sublimation pump. The limiting vacuum obtained after 48 h baking at 200 °C is 8×10^{-11} Torr. The chamber is equipped with two ionization gauges and a residual gas analyzer (quadrupole mass spectrometer). It is connected to two independent gas introduction lines. The partial pressure of the gases introduced in the chamber can be either monitored or controlled, this being particularly useful for adsorption kinetics studies.

A (140—600)-V ion gun is used for sample cleaning. The samples can be studied with standard surface techniques using a vertically translatable four-grid LEED-Auger system provided with a transparent screen. This feature was required since the sample holder is large, and hence the observation of the LEED patterns is much easier and precise from the electron-gun side. Two electron guns are available, one 5—3000 V, 10 μA in the axis of the screen for LEED and another 100—3000 V, 150 μA at grazing incidence (12°) for Auger measurements.

Many ports on the chamber can be used for viewing and for the installation of further equipment such as evaporation systems. A very wide aperture on the bottom of the chamber can also be provided with a complex evaporator, which is currently being studied. One of the ports is equipped with a deep well in which a photomultiplier can be placed, allowing x-ray detection with a sufficient solid angle.

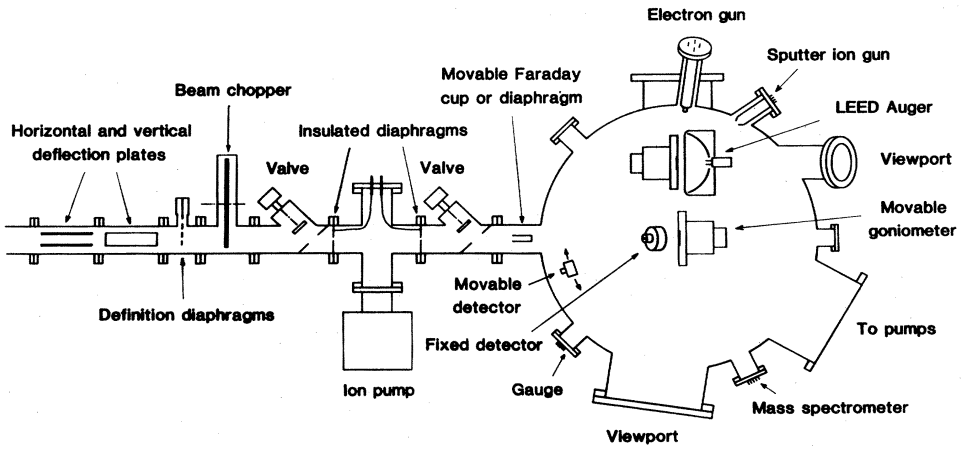

FIG. 1. Ultra-high-vacuum chamber and connected beam line.

B. Goniometer

The goniometer of the UHV system is represented in Fig. 2. It has three rotation axes ($\pm 145°$ and $\pm 15°$ excursion). The three rotation axes intersect on the sample surface. The reproducibility in position for the three movements after backlash compensation is of the order of 1—3′. A Z (horizontal) translation of 8 cm and an X (vertical) translation of ± 8 mm (the latter by using an external rod) are available. The large tilt excursion of $\pm 145°$ combined with the large X translation allows the sample to be moved from a position corresponding to the LEED-Auger analysis to a position in front of the accelerator beam. When necessary, the rotation movements can be driven by stepping motors and controlled by the on-line computer, together with the entire setup linked to the accelerator.

The sample holder is sufficiently electrically insulated from the manipulator to allow the measurement of electron beam and sputtering ion beam currents. The sample holder is also thermally insulated and the sample can be heated up to 800 °C by a resistor or up to 1000 °C by electronic bombardment of the back side of the sample. A cooling system is being completed which will enable the sample to be cooled down below 150 K. The temperature is measured by a thermocouple clamped in a hole in the sample edge.

C. Standards

When the manipulator is moved out of the accelerator beam, it can be replaced by a Faraday cup to measure the beam current, or by a set of reference targets in the same position as the sample to calibrate Rutherford backscattering or nuclear reaction measurements. The holder of the Faraday cup and reference targets can be translated in the X (vertical) direction by a magnetic handle. For the present experiments four standards were settled in the chamber: (i) a backscattering standard consisting of a thin Ta deposit on Si, known with a precision of $\pm 2\%$ (Ref. 3); (ii) an ^{16}O and an ^{18}O standard consisting of thin Ta_2O_5 oxide layers on Ta formed by anodic oxidation, respectively, in ordinary or ^{18}O-enriched solutions, the ^{16}O and ^{18}O contents being known, respectively, with a 3% and $\pm 5\%$ precision;[4] (iii) a ^{12}C standard obtained by ion implantation of $\simeq 10^{17}$ ^{12}C atom/cm^2 in Ta and known with a $\pm 8\%$ precision.

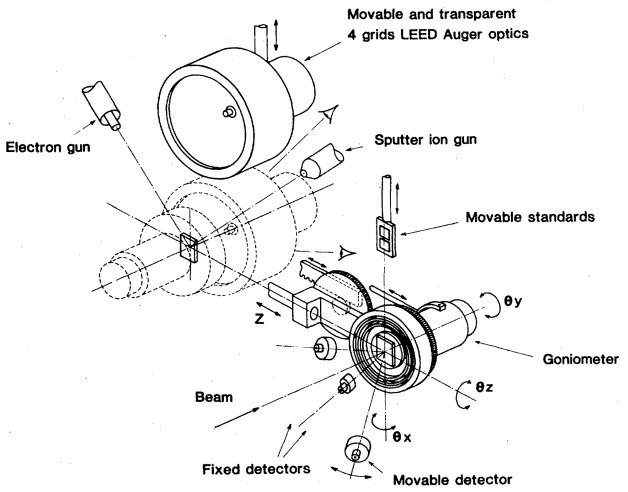

FIG. 2. Goniometer and facilities inside the ultrahigh-vacuum chamber.

D. Detection

The chamber is equipped with three surface-barrier detectors. Two detectors are at fixed positions at 7 and 5 cm from the sample. The first one (25 mm^2) is used for backscattering measurements at $\theta_{lab}=165°$. The second (300 mm^2) at $\theta_{lab}=150°$ is used for nuclear reactions. Various absorbers of different thicknesses (used to stop the backscattered particles and avoid pile-up problems for nuclear reaction analyses) and a mask, protecting the detector during sample annealing, can be placed in front of these detectors by using an external handle. The third detector is mobile and is placed 15 cm from the sample. It is equipped with a small ($\simeq 1$ mm^2) diaphragm in order to have a good detection-angle definition and to perform blocking experiments. For these experiments the beam impact diameter also never exceeded 1 mm^2. The detection angle can be varied in a horizontal plane from 85° to 170°, the absolute angle between the incident and detected beams being known for all detector positions with a 3′ precision. This value corresponds to the reproducibility obtained after detector rotation.

The three detectors are standard surface barriers from Ortec. They are therefore not bakable. However, all three are inserted in a copper block cooled by liquid circulation. During chamber baking at 200 °C, a water circulation was sufficient to maintain the detector temperature at 50 °C. During experiments, degasing from the detector has been shown to have a negligible influence on sample surface pollution. The main advantage in using standard instead of bakable detectors is the much better energy resolution obtained (10 keV instead of 30 keV for backscattering experiments).

E. Beam dose measurements

Between the UHV chamber and the accelerator line in which the vacuum is $\simeq 10^{-7}$ Torr, a differential pumping section limited by two 3-mm^2 diaphragms, equipped with an ionic pump, reaches a vacuum of a few 10^{-9} Torr. The UHV chamber is not sufficiently insulated to obtain a reliable integration of the beam current. In order to measure the beam dose, the accelerator line is equipped with a beam chopper[5] consisting of a rotating sector with two blades which intercept about 20% of the beam. The blades consist of an aluminum substrate covered by a $\simeq 1000$ Å thick gold deposit. The beam dose is monitored by measuring the number of particles backscattered from this gold layer which hit a surface-barrier detector.

A set of horizontal and vertical deflection plates placed on the beam line before the differential pumping section allows us to adjust the beam trajectory and ensures that the entire beam passes through the two diaphragms of this section: this is checked by the fact that no current is measured on these diaphragms (which are electrically insulated).

III. Cu SAMPLE

A. Sample preparation

A (100) copper single crystal has been grown with the use of the Bridgman method from a Cu bar of high purity (overall amount of impurities $\simeq$10 ppm). The monocrystalline bar was then cut in $\simeq$4 mm thick slabs, the surface orientation of the slabs being 5° off the (100) plane in the $[0\bar{1}1]$ zone axis. The slice orientation, (16,1,1) using the Miller notations, was controlled by Laue x-ray diffraction with a precision better than 1°. After cutting, the samples were first mechanically, then electrolytically polished. The latter treatment was performed under 1.8 V for 30 min in an aqueous solution containing 60% H_3PO_4. This procedure removes the defects induced by the mechanical polishing and provides a well-ordered surface.

The sample treatment in the UHV chamber consists of argon bombardments at 400 eV with a 4-μA current. The Ar beam hits the surface under 45° incidence. The bombardments are followed by 10-min annealing at 600 °C. During argon bombardment, argon is introduced in the chamber at a 5×10^{-5} Torr pressure. The ionic and turbomolecular pumpings are stopped but the trap is kept at liquid-nitrogen temperature in order to lower the contaminant (mainly CO and H_2O) partial pressure. A titanium sublimation is also performed before argon introduction. The bombardments last approximately 10 min and during this time the sample temperature is gradually increased from 30 to 300 °C. The H_2O and CO partial pressures reached at the end of the bombardment are of the order of a few 10^{-9} Torr. This is 20—50 times larger than the pressure during LEED-Auger or ion-beam analysis measurements. The main contamination of the sample surface therefore takes place immediately after argon bombardments. This is confirmed by the fact that there is no marked evolution of the Auger spectra even after a long set of ion-beam analysis measurements. The Auger analysis reveals only one impurity: a very small carbon peak at the limit of the measurement sensitivity. No sulfur segregation towards the surface is noticed, since the sample is not heated above 700 °C for a significant time. Also, up to 700 °C, no blistering problems related to the ^{4}He beams used in channeling experiments occur. These problems do become serious above 700 °C.

B. Sample characterization

The oxygen and carbon content of the crystal surface region have also been measured by nuclear microanalysis using the $^{16}O(d,p)^{17}O^*$ and $^{12}C(d,p)^{13}C$ nuclear reactions and the standards described in Sec. II C for calibration. The detected quantities were, respectively, in the $(3-5)\times10^{13}$ ^{16}O atoms/cm^2 and $(5-8)\times10^{13}$ ^{12}C atoms/cm^2 ranges, i.e., 2—3% and 3—5 % of an atomic plane of Cu [1.53×10^{15} Cu atoms/cm^2 in a (100) plane]. The measurements were performed using a 100-nA. deuteron beam and the counting rates were approximately 0.1 and 1 sec^{-1} for ^{16}O and ^{12}C. No significant variation of the contamination was observed when comparing consecutive countings, therefore the contamination introduced during accelerator bombardment is small. Since the energy resolution associated with the nuclear reaction analyses corresponds to a depth resolution of a few thousand Å, the measured C and O could originate both from the surface and from bulk contamination. However, since the solubility limits for C and O in Cu are in the ppm range, the volume contribution is probably negligible and the quantities measured correspond, unfortunately, to surface contamination.

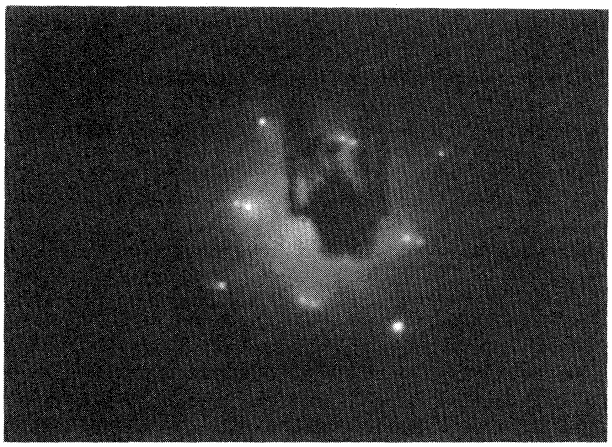

FIG. 3. LEED pattern on a clean (16,1,1) Cu surface. The double spots are characteristic of the stepped structure. Electron-beam energy: 123 eV.

The LEED patterns exhibit, at characteristic energies, double spots typical of the stepped structure.[6] This feature is due to constructive interferences corresponding to electrons diffracted by consecutive atoms *and* by consecutive terraces. The distance between the two spots of a doublet is therefore characteristic of the terrace widths. The energies at which the double spots are observed are characteristic of the step height. The sharpness of the spots is indicative of the sharpness of the terrace-width distribution. In our case the double spots were rather broad, showing that the terrace widths were distributed between 6 and 10 atoms along the [011] axis perpendicular to the terrace edge. The width (determined by the cutting angle) corresponding to terraces of assumed equal size would be eight atoms. The height of a step corresponds to one (100) interplanar distance.

A typical LEED pattern with the doublets characteristic of the (16,1,1) stepped surface is presented in Fig. 3. This photograph corresponds to the sample used in our experiments but was taken in another UHV chamber, where the contrast was better.

C. Measurement of saturation oxygen coverage

In the experiments where the influence of oxygen coverage was studied, the sample, after sputtering and annealing, was treated at 300 °C under a pressure of 5×10^{-5} Torr of oxygen. These conditions were demonstrated to lead to saturation coverage Θ_s. Measurements of the saturation oxygen coverage on Cu(100) have been undertaken by other authors in Ref. 7 by Auger analysis after oxygen and Pb coadsorption. They found $\Theta_s=0.75$. Since the LEED pattern indicates that the adsorbed oxy-

gen has the $(2\sqrt{2}\times\sqrt{2})R45°$ symmetry, this value of Θ_s corresponds to three oxygen atoms per mesh. In our experiments the number of oxygen atoms measured by the $^{16}O(d,p)^{17}O^*$ reaction corresponds to 7.6×10^{14} cm^{-2}, i.e., to $\Theta_s=0.5$. The difference between the two results may have various origins. It could be due to, in particular, the different measuring techniques used. On the one hand, the absolute amounts obtained from the Auger measurements may be questioned, particularly in the case of the results of Ref. 7, where Θ_s was obtained rather indirectly via measurements of the Pb coverage in the sites left free by oxygen. On the other hand, some oxygen desorption during the $^{16}O(d,p)^{17}O^*$ measurements cannot be excluded, but this effect is expected to be small, since we have found that the oxygen quantity measured did not vary significantly for successive measurements, i.e., when increasing the beam dose. In any case, there is no major reason for which the desorption due to the deuteron beam should be significantly higher than the one induced by the electron beam during Auger measurements.

Another explanation for the discrepancy may be related to the fact that we are studying a vicinal surface. A LEED diagram obtained after oxygen adsorption is presented in Fig. 4. This pattern is characteristic of surface reconstruction and faceting, in agreement with previous results.[2] The faceting process is schematically shown in Fig. 5. The surface is now formed of (100), (410), and (401) domains. The (410) stepped structure corresponds to (100) terraces with a width, along the [011] axis, half as large as in the (16,1,1) case. This therefore implies that the overall area of the (410) and (100) domains must be equal in our case. Consequently, the oxygen coverage measured should be the average of coverages corresponding to (100) and (410) structures. The comparison of Auger O/Cu signal-intensity ratios for (100) and (410) surfaces has been recently undertaken in our laboratory for exposures at 600 K.[8] The results demonstrate that the oxygen saturation coverage for (410) is about half as large as that for (100). Assuming the (100) coverage to be 0.75, this result would imply that the saturation coverage for our (16,1,1) Cu surface is about 0.56, which is in good agreement, within experimental uncertainties, with our nuclear reaction measurements.

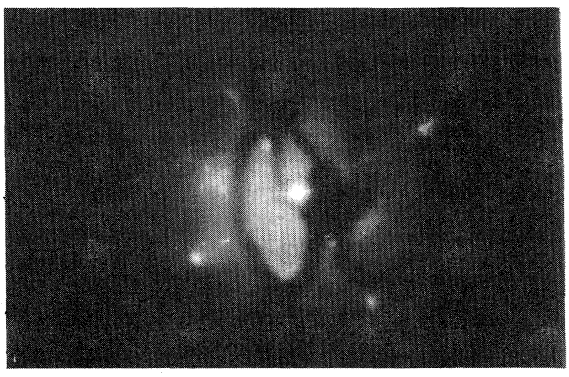

FIG. 4. LEED pattern on the sample after oxygen adsorption at saturation coverage. This diagram is characteristic of faceting in (100), (410), and (401) domains. Electron-beam energy: 114 eV.

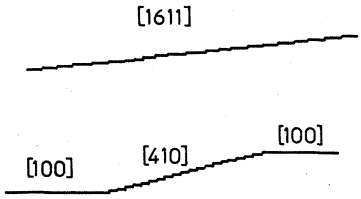

FIG. 5. Schematic of the faceting process induced by oxygen adsorption.

IV. CHANNELING ON STEPPED SURFACES: POSSIBLE EXPERIMENTS AND EXPECTED RESULTS

It is of interest to note that in most channeling experiments the surface orientation of the crystal studied is considered as satisfactory as long as this orientation is less than 2°—3° off a major plane. In such a situation, assuming that the stable surface configuration corresponds to large domains of the close low-index plane orientation, the misorientation must be compensated in some way by the presence of surface defects such as adatoms, advacancies, irregularly spaced steps, etc. These features are generally not considered when interpreting channeling experiments. When the angle between the surface and a major plane is increased, an organization in periodic steps with quasi-equal terrace widths is easier to achieve; this is the case in our experiments.

The (16,1,1) crystallographic structure is schematized in Fig. 6. The specific channeling experiments that can be performed on such structures will be presented in Sec. IV B. Section IV A will precede with a discussion of the more standard channeling experiments that we have also undertaken in order to measure the surface relaxation.

A. Search for surface relaxation by "standard" channeling experiments

Reliable theoretical predictions about lattice relaxation at metal surfaces are very difficult to obtain, since strong assumptions about crystal potentials are required in the calculations. For instance, the very nature of pair potentials systematically leads to the prediction of an expansion of the first interlayer distance. For the Cu(100) surface which is of interest in the present work, an expansion of 8.6% has been calculated with the assumption of Morse—or Lennard-Jones—type potentials.[9] On the contrary, in the case of oscillatory potentials, contraction ef-

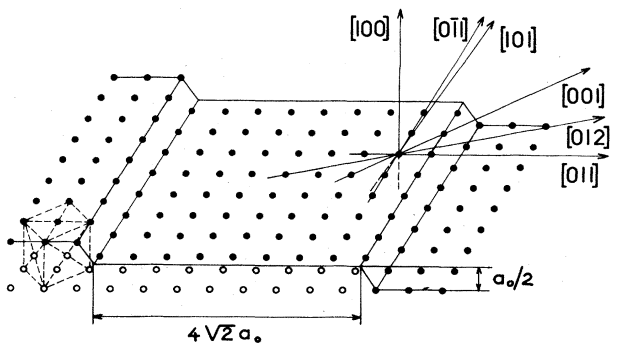

FIG. 6. Schematic of the (16,1,1) stepped structure.

fects are often found. In Ref. 10, with the use of a tight-binding model for the transition metals, a contraction of 9.2% for the same Cu(100) surface was calculated. An electrostatic model developed in Ref. 11 predicts, still for Cu(100), from 2.4% contractions up to 3.7% expansions, depending on the electronic densities introduced. The latter calculation, which finds rather small relaxations is at least in agreement with LEED measurements.[12] It may be noticed that the calculations of Ref. 11 predict much stronger effects for the Cu(110) surface. Whatever electronic density considered, a strong contraction of the first interlayer spacing and a strong dilatation of the second are calculated. LEED and channeling measurements on Cu(110) seem to agree with this conclusion.[13]

In this work we have studied the relaxation of the (100) terraces. The channeling technique is particularly well adapted for relaxation measurements, since such an effect corresponds to a coherent displacement of a whole atomic plane. Therefore, the problem is the determination of a single lattice site or at most two sites if, as in the case of Cu(110), the relaxation of the second layer is also significant.

Two types of channeling measurements can be performed. The first type consists of studying the symmetry of an axial angular scan corresponding to the surface-peak integral in single-alignment geometry with respect to an axis which is not normal to the crystal surface. The main problems in this technique arise from background subtraction under the surface peak. Improvements can be obtained by detecting particles backscattered at grazing emergence, but still, the background becomes large when the angle between the beam and the crystallographic axis increases. This introduces serious difficulties: since the dip symmetry is under study, rather large angular excursions are required and the background problems are unavoidable.

We have hence preferred a second technique, developed by Turkenburg, Smeenk, and Saris,[14] in which the symmetry of blocking dips in double-alignment geometry is studied. The incident beam remains parallel to the [100] axis perpendicular to terrace plane and the surface-peak integral is studied as a function of the detection angle with respect to the [101] axis at 45°. The geometry of the experiment is schematized in Fig. 7. In such a study, the background subtraction problems are no longer crucial, the background remaining low even for large changes in detection angle. However, other difficulties arise. They are related to the fact that the surface-peak integrals do not change markedly when the detector is tilted from double to single alignment. For instance, assuming that there is no surface relaxation and neglecting correlation effects, we find the surface peak is about twice as high in single alignment as in double alignment. The real contrast is in fact significantly smaller due to correlation effects which can in no way be neglected in double alignment: A backscattered particle has a high probability of having hit a rather strongly displaced atom (this displacement being either static or dynamic, i.e., thermal vibrations), and consequently the blocking effect on the way out will be poor. Moreover, if the relaxation searched for is really significant, it will further lower the contrast. This means that in order to substantiate the dip shape, good statistics are needed. These statistics require high beam doses, due to the small detection solid angle used for the blocking experiments, and damage problems may arise (see Sec. IV C).

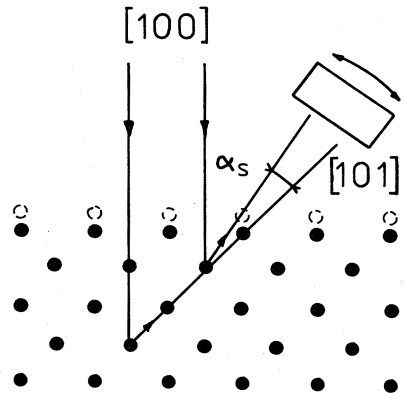

FIG. 7. Principle of surface-relaxation measurements in double-alignment geometry. The angle α_s is of the order of the shift of the bottom of the surface dips. These dips are also asymmetrical.

However, most of these problems can be minimized, and the situation seems to remain more favorable than in the single-alignment experiments, if the choice of the beam energy is optimized. At too-low beam energies there is a marked loss in sensitivity to atomic displacements. However, the sensitivity remains sufficient at energies sufficiently low to correspond to high Rutherford cross sections and avoid damage problems that are too serious (see Sec. IV C). The energy also must be chosen sufficiently low in that the contribution to the surface peak of the first two atomic planes, between which the relaxation is measured, becomes dominant. This is the case of our experimental situation where 200-keV ^{4}He was chosen. For such beams the contribution of the third atomic plane becomes small. Since there is no shadowing effect of the first atomic plane on the second one for the incoming beam, we are mainly dealing with a pure blocking experiment (see Fig. 7). Therefore, no correlation effects between the incoming and outgoing trajectories must be taken into account. Our beam-energy choice seems to be a good compromise. Use of lower ^{4}He energies would affect the precision of our relaxation measurements. The angular scattering for 200-keV ^{4}He is the same as for the 100-keV H^+ often used by Turkenburg, Smeenk, and Saris.[14] Our choice of ^{4}He beams instead of protons is related to the higher stopping power for ^{4}He and the associated improved depth resolution. The use of proton beams requires a very good energy resolution, i.e., detection with an electrostatic analyzer as performed by Turkenburg, Smeenk, and Saris.

The surface relaxation is expected to be very sensitive to surface coverage. In the case of Ni, channeling studies[15] indicate that while surface contraction is observed on an uncovered surface, surface expansion is seen when oxygen is adsorbed at saturation coverage. In the present work, we have therefore undertaken relaxation studies for these two situations.

We have also undertaken systematic single-alignment studies along the [100] axis perpendicular to the terraces as a function of beam energy in order to check if such a technique is sensitive to the surface disorder and thermal vibrations.

B. "90°" double-alignment studies: Structural information on the first atomic layer

The geometry of the experiments is as follows. The incident beam is always parallel to the [100] axis perpendicular to the terraces, and we detect the particles backscattered at 90° along a crystallographic axis in the terraces. The alignment of the incident beam is only achieved in order to lower the background. A typical experiment is schematized in Fig. 8. Assume, for given experimental conditions, that the number of atoms per row corresponding to the surface peak for the blocking direction $[hkl]$ studied in the terraces is $N_{(hkl)}$, and call $N_{T(hkl)}$ the number of atoms per row, along the same direction, corresponding to a terrace width. The surface peak will represent a number of atomic planes equal to the ratio $N_{(hkl)}/N_{T(hkl)}$. In practical cases, this ratio is often significantly smaller than 1. The surface peak thus represents less than one atomic plane. If the height of the steps corresponds to one interplanar distance, which is the case of our experiments as demonstrated by the LEED patterns, this means that the surface peak originates only from particles backscattered by atoms of the very first atomic layer and therefore provides exclusive information about the crystallographic structure and thermal vibrations of this layer. The particles backscattered on the second layer are deflected by the N_T atoms of the first terrace and cannot reach the detector aligned with the $[hkl]$ direction. If, on the contrary, the height of a step represents two interplanar distances, particles backscattered at 90° on the second layer can leave the crystal without being deflected by atoms of the first layer and they will therefore contribute to the surface peak, even with $N/N_T < 1$. This was never the case in our experiments.

1. Study of the step-edge atoms

If the detection direction is aligned with the [011] or the [001] axis in the terraces (respectively, at 90° and 45° of the terrace edges), we are dealing with a situation where all the axes begin by an edge atom (see Fig. 6). If the experiments are performed with ^{4}He beams, the number of atoms per row N as calculated by a Monte Carlo simulation (taking into account the particle energy after backscattering, assuming a perfect crystalline order and surface vibrations identical to bulk vibrations) is, respectively, 1.70 for [011] and 1.45 for [001]. The contribution of the edge atoms to the surface peak is hence predominant and their position can be studied with high precision.

For instance, a possible relaxation of the step-edge atoms perpendicular to the (100) terraces can be evidenced by studying the symmetry of angular scans giving the surface-peak integral when the detector is moved out of the [011] direction, perpendicularly to the terraces. The experiment is schematized in Fig. 9(a). The principle is exactly the same as for the study of surface relaxation described in Sec. IV A. The relaxation of the edge atoms in the terrace plane, perpendicular to the terrace edge, can be studied by angular scans around the [010] axis at 45° of this edge. In such an experiment, schematized in Fig. 9(b), the detector is kept fixed at 90° of the incident beam and the crystal rotated in its own plane. Here again, as in the relaxation studies of Sec. IV A, an asymmetry and a shift in the angular position of the surface dip minimum with respect to the bulk dip minimum, should be observed.

It must be pointed out that since the edge atoms are particularly loosely bound, such relaxations may be expected. Low-energy ion scattering experiments reported in Ref. 16 find a strong vertical contraction of the interlayer spacing $(10\pm3)\%$ in the vicinity of the step edge for

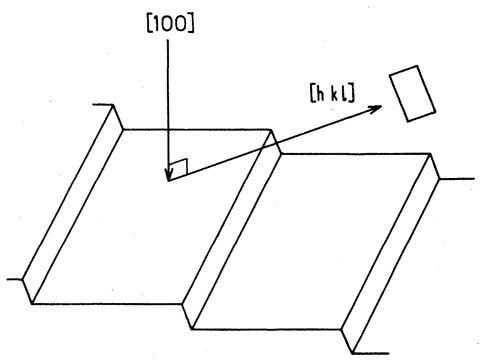

FIG. 8. 90° double-alignment geometry.

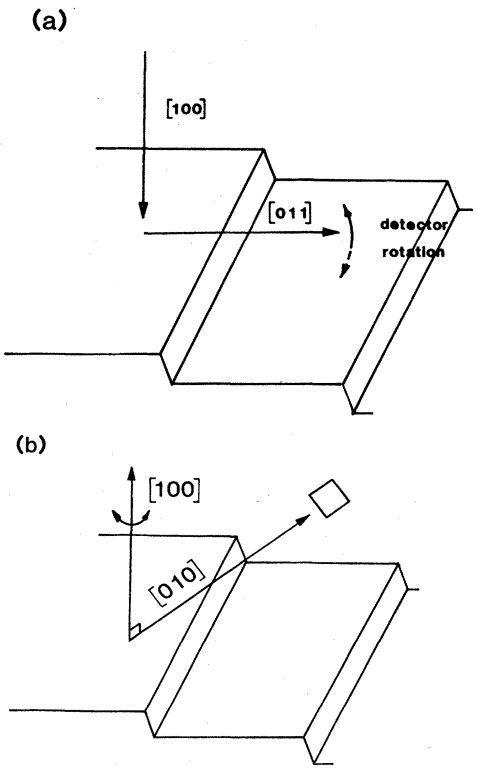

FIG. 9. (a) Principle of measurement of vertical step-edge relaxation. (b) Principle of measurement of edge-atom relaxation, inside the terraces, perpendicular to the step edge.

(410) terraces. Note that in these experiments the mean interlayer spacing is found approximately equal to the bulk interplanar distance. The results of Ref. 16 therefore seem to indicate a specific edge-atom relaxation.

Once the mean position of the edge atoms has been determined, the minimum value of the surface-peak integral provides information about surface vibrations. The surface atoms are expected to have enhanced vibrations as compared to bulk atoms, particularly perpendicular to the surface. The effect is expected to be significant. For instance, the surface Debye temperature predicted from the calculations of Ref. 17 for various copper surfaces is approximately 230 K instead of 350 K for the bulk. The more loosely bound edge atoms are expected to vibrate even more. Of course, in order to obtain precise information, the correlation of thermal vibrations must be taken into account, since it may affect the surface-peak yield.

2. *Study of surface atoms inside the terraces*

The edge atoms are in a singular situation. The atoms inside the terraces are, in a first approximation, in the same configuration as atoms of a pure (100) surface, a second-order effect being a possible influence on these atoms of interactions between step edges. Hence their study is of general interest. It can be performed by experiment on secondary axes in the terraces. Generally, such axes do not contain mostly step-edge atoms. For instance, in the case of the [012] axis which is studied in this work, only one of three axes contains a step-edge atom (see Fig. 6). For these axes the value $N_{T[012]}$ of atoms per terrace is 3. This is markedly higher than the number of atoms per row corresponding to the surface peak which is, for instance, only 1.1 at 200 keV and 1.5 at 500 keV (assuming a perfect order and bulk thermal vibrations), due to the great interatomic distance. Hence again the surface peak corresponds to atoms of the very first layer, but this time those atoms inside the terraces, and will provide information about surface order and surface vibrations. It is interesting to note that since the consecutive atoms along [012] are not very near neighbors, their thermal vibrations are not expected to be strongly correlated. A comparison between results for low- and high-index axes should therefore improve our knowledge of the correlations.

It is well known that the number of atoms per row corresponding to the surface peak is a function of the parameter ρ/R, ρ being the rms thermal-vibration amplitude perpendicular to the axis, and R is the radius of the shadow cone after one interatomic distance. R is a function of beam energy (varying roughly like $E^{-1/2}$). Information about surface order and thermal vibrations is hence provided by studies of surface-peak integrals as a function of crystal temperature and beam energy. In standard channeling experiments, however, such studies are limited by the fact that the number of atoms seen per row must remain small in order to obtain information about the surface plane. This is not the case in 90° double-alignment experiments in which, for example, if the number of atoms seen per row is small with respect to 8 in the [001] or [011] direction, the surface peak originates only in the first surface plane. Beam energy and crystal temperature can hence be varied in a wide range.

3. *Study of surface structure under oxygen coverage*

We have indicated in Sec. III C that when oxygen is adsorbed at the saturation coverage, the LEED patterns show faceting with the presence of both (100) and (410) domains, each domain occupying half of the surface. The fact that the faceting is seen in LEED indicates that the size of the domains exceeds 100 Å (i.e., the coherence length).

In such a situation the contribution of the (100) domains to 90° double-alignment spectra will be negligible, and the results will provide information about the (410) surface structure when covered by oxygen. If the oxygen adsorption does not induce surface disordering, the surface-peak integrals are expected to be the same as for uncovered surfaces. This is due to the fact that the ratio N/N_T for the (410) is double that for the (16,1,1), since the number of atoms per row seen in channeling, N, is constant, and the number of atoms in a terrace along the direction studied, N_T, is twice as small for (410) domains. Since these domains occupy only one half of the surface, and since the contribution of the (100) domains is negligible, the surface peak will correspond to $1/2(N/N_T)_{(410)}$, i.e., $(N/N_T)_{(16,1,1)}$.

If, on the contrary, oxygen adsorption induces disorder, the surface-peak integrals will increase. We have checked if such a disordering occurs by comparing 90° double-alignment results before and after oxygen adsorption.

C. BEAM DAMAGE IN DOUBLE-ALIGNMENT EXPERIMENTS

The problem may be summarized in the following terms. The aim is to obtain, with sufficient statistics, a surface peak corresponding to backscattering on roughly the first atomic plane, the detection solid angle being restricted by the blocking geometry. Call T_{th} the threshold energy transfer in one collision leading to the displacement of an atom. An impact parameter p_{th} is associated with T_{th}. The number N_d of displaced atoms in an atomic plane (neglecting displacements by secondary collisions) is related as follows:

$$N_d \propto p_{\text{th}}^2 \Delta \,, \tag{1}$$

where Δ is the beam dose.

Assuming for the sake of simplicity that the Rutherford cross section holds, one has

$$p_{\text{th}}^2 \propto \frac{M_1}{M_2}\frac{b^2}{T_{\text{th}}}E, \quad M_1 \ll M_2 \tag{2}$$

where M_1 and M_2 are the atomic masses of the incoming ion and the target atoms, b is the collision diameter (minimum distance of approach in a collision with impact parameter $p=0$), and E is the beam energy.

The beam dose Δ required to accumulate a given amount of statistics is related as follows:

$$\Delta \propto \frac{1}{\sigma\, d\Omega} \tag{3}$$

where σ is the Rutherford cross section at the backscattering detection angle θ, and $d\Omega$ is the detection solid angle.

The angular aperture of detection must be small with respect to some characteristic blocking angle ψ_c and hence, $d\Omega$ is related as follows:

$$d\Omega \propto \psi_c^2 \propto \frac{M_1 M_2}{E} . \tag{4}$$

The cross section σ is related as follows:

$$\sigma \propto \frac{b^2}{\sin^4(\theta/2)} . \tag{5}$$

Finally,

$$\Delta \propto \frac{1}{\sigma\, d\Omega} \propto \sin^4\left(\frac{\theta}{2}\right) \frac{E}{M_1 M_2} \frac{1}{b^2} \tag{6}$$

and

$$N_d \propto p_{\text{th}}^2 \Delta \propto \frac{1}{T_{\text{th}}} \sin^4\left(\frac{\theta}{2}\right) \frac{E^2}{M_2^2} . \tag{7}$$

Assuming that T_{th} is not strongly dependent on the material (it is of the order of 5 eV for surface atoms and 20 eV for bulk atoms), the relation (7) demonstrates that backscattering experiments can be performed with markedly less damage to heavy than light targets. But the most interesting feature is the energy dependence of N_d. The damage is minimized by lowering the beam energy. In particular, it is not correct to present, as is often done, high-energy backscattering as a less destructive technique than low-energy backscattering. The main advantage of high energy is mostly its better sensitivity to small atomic displacements (and also the fact that it provides more quantitative results). As analyzed in Sec. IV A the better compromise in term of sensitivity corresponds to 200-keV ^{4}He or 100-keV H^+ From the point of view of damage, 100-keV H^+ bombardment induces 4 times less disorder than 200-keV ^{4}He, but the use of an electrostatic analyzer is required.

In the case of single-alignment experiments, due to the large detection solid angle used, the beam doses required are small, and the damage induced is negligible. On the contrary, in the cases of double alignment, even in the most favorable situation (200-keV ^{4}He) used in this paper, an angular scan (i.e., about 10 spectra) requires an overall dose of 50–100 μC. If the entire scan is recorded with the beam on the same impact point ($\simeq$1 mm^2), such a dose represents about 25% of displaced atoms on an atomic plane if one assumes a displacement energy threshold $T_{\text{th}}=5$ eV, and about 7% if one assumes $T_{\text{th}}=20$ eV (bulk value). These values, calculated with a Thomas-Fermi–type potential for the ion-atom interaction, are very high. However, in our experiments, we never noticed an influence of beam damage on the results: surface peak integrals before and after an overall angular scan were always found identical. Therefore, we must assume that for the temperature at which the experiments were performed (300 and 600 K) spontaneous beam-damage annealing takes place. This is confirmed by the fact that after surface sputtering by 500-eV Ar beams, surface reordering is observed by LEED in a few minutes at room temperature. We cannot exclude the possibility that beam damage will be a serious problem for low-temperature double-alignment experiments that we plan to perform in the near future.

V. MONTE CARLO SIMULATIONS

The experimental results were compared to Monte Carlo simulations. Since in most cases in our experiments the number of atoms per row corresponding to the surface peak is small, a single string approximation has often been considered as sufficient. This approximation becomes questionable, however, when angular scans are simulated and hence that the surface yield at rather large tilting angles is calculated. Most of the angular dips correspond to axial-planar transitions. We have, when necessary, simulated such dips, taking into account the near-neighbor rows with their position and direction. For this purpose, particles reaching the border of the unit cell associated with the main string studied are reflected inside the cell with reflection conditions accounting for the other strings.

The main weakness of our simulations is that correlations in atomic displacements cannot be accounted for. As a matter of fact, we calculate the particle flux in a unit cell for a given incident-beam direction. Assuming axial symmetry and letting $\vec{r}$ be a vector in the transverse plane (with respect to the string), we write that the yield Y_i corresponding to the ith string atom and normalized to the random yield is given by

$$Y_i = \frac{\int_0^{r_0} 2\pi r f_i(\vec{r}) g_i(\vec{r}) dr}{\int_0^{r_0} (2\pi r/\pi r_0^2) g_i(\vec{r}) dr} , \tag{8}$$

where r_0, radius of the unit cell, is defined by the relation $\pi r_0^2 = (Nd)^{-1}$. d is the interatomic distance, and N is the number of atoms per cm^3. $f_i(\vec{r})$ in relation (8) is the particle flux in the transverse plane associated with the ith atom which results from the Monte Carlo simulation. $g_i(\vec{r})$ is the distribution of the ith atom, taking into account thermal vibrations. We neglect here the atomic displacements in the string direction. The denominator in Eq. (8) corresponds to the random yield, meaning that our definition for random is that the particle flux in the unit cell is uniform.

Of course, in relation (8), the flux distribution $f_i(r)$ could have been calculated by taking into account correlations in thermal vibrations in the Monte Carlo simulation. But this would not be sufficient. The point is, as demonstrated in Ref. 18, if correlations must be considered, relation (8) itself is not valid. The knowledge of the flux is no longer sufficient to predict the backscattering yield for a given atom: As the atomic displacements are correlated, the yield will depend on the particle history. A cross section must be defined, and the close-encounter probability must be determined particle by particle. Such a simulation is not more difficult than the one performed using relation (8); it only requires much longer computing times, and we could not undertake it in our present situation. Much more sophisticated simulations, taking into account correlations, have been undertaken in other laboratories.[18]

Correlation coefficients between two consecutive vibrat-

ing atoms along a string have been calculated.[19] A transition is observed around the Debye temperature Θ_D. For $T \ll \Theta_D$ and $T \gg \Theta_D$, two constant values are obtained, the correlation being markedly stronger at high temperature. In the case of fcc metals (the case of Cu) and for the [110] axis, the correlation coefficients are, respectively, near 0.14 and 0.36 at low and high temperature. The Monte Carlo simulations performed in Ref. 18 indicate that for correlation coefficients around 0.3, the surface-peak integral is about 15% lower than for uncorrelated vibrations. The Debye temperature for Cu being around 350 K, the correlation effects on surface peaks in our case are expected to be of the same order of magnitude.

We have also developed a program corresponding to blocking simulations. The factor of interest is that a whole angular scan can be calculated in one step. As indicated in Sec. IV B, many of our measurements correspond to blocking experiments. Lindhard has stated,[20] that, due to statistical mechanics considerations, reversibility between channeling and blocking applies in a general way. However, it does not appear obvious how to demonstrate analytically that reversibility holds for surface-peak calculations, i.e., without assuming a flux distribution corresponding to statistical equilibrium. As a matter of fact, the comparison of our channeling and blocking simulations indicates that reversibility fully applies. Any of these simulations can hence be compared, when convenient, indiscriminantly to our experiments.

In the 90° double-alignment experiments, since the surface peak originates only from the first atomic plane which is seen in the same way regardless of the incident-beam direction, the associated calculations must correspond to single alignment. For "true" double-alignment experiments our simulations clearly do not hold. The calculations are difficult, owing to the fact that particle trajectories in the ways in and out are not independent (see Sec. IV A). However, in the experimental situation described in Sec. IV A, near the dip minimum we are again in a single-alignment (blocking) case. Of course, this is not true for the calculation of the whole dip, which has not been undertaken in the present work.

The particle fluxes $f_i(\vec{r})$ have been calculated using the Moliere approximation of the Thomas-Fermi potential[21] for scattering calculations. The latter were performed in the small-angle approximation, and energy losses were neglected. We have checked our program by comparing our results, for the number of atoms per row corresponding to a perfectly aligned beam in a perfect crystal as a function of the parameter ρ/R, to already published calculations.[22] The agreement is satisfactory.

We have attempted to predict the effect on angular scans of static displacements of the first atom of a string, perpendicular to the string direction. These simulations are indicative of the expected effects either of surface atoms, or simply of edge-atom relaxation, according to the experimental configuration. The simulations were performed for 200-keV ^{4}He ions on a crystal at 300 K and with the assumption of a surface thermal vibration identical to the bulk-atom vibration extracted from the Debye temperature (i.e., $u_x = u_y = u_z = 0.085$ Å at 300 K). The lattice parameter for Cu is 3.615 Å. Displacements of

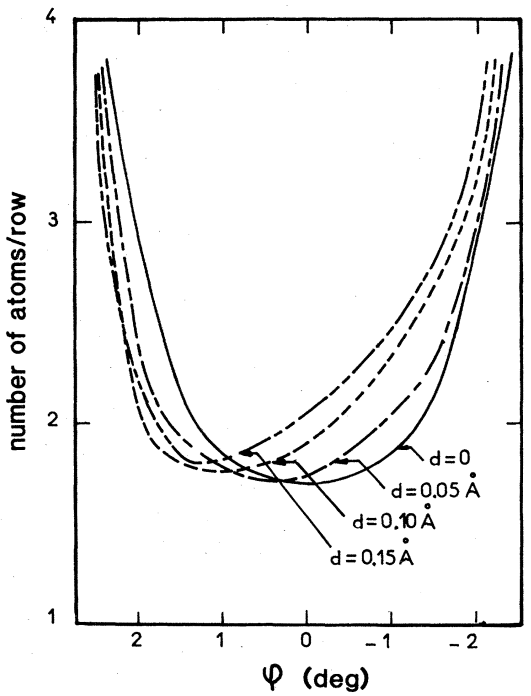

FIG. 10. Monte Carlo simulations of angular scans across the [110] axis, indicating either overall surface relaxation, or step-edge relaxation, owing to the experiments. d is the amplitude of the relaxation assumed. The simulations correspond to 200-keV ^{4}He ions. The surface and bulk vibrations were assumed equal ($u_B = 0.085$ Å).

0.05, 0.1, and 0.15 Å were introduced. The calculated angular scans of Fig. 10 are relative to the [110] axis and should hence be compared either to [100]→[101] double-alignment experiments at 45° to check the surface plane relaxation, or to [100]→[011] alignments at 90° to check the step-edge atoms relaxation perpendicular to the terrace plane (see Sec. IV B). We have also calculated scans relative to the [100] axis which are to be compared to [100]→[001] alignments at 90° to check step-edge atoms relaxation in the terrace perpendicularly to the terrace edge. The scans reported in Fig. 10 indicate that a relaxation of the order of 0.05 Å (i.e., about 3%) is close to the sensitivity limit (taking into account the expected experimental uncertainties), but appears still to be measurable.

The calculated scans have also allowed us to account for the effect of incident-beam divergence (always negligible in our experiments) or of angular acceptance of the detector in blocking experiments (which may be significant when rather high index axes are studied). We could therefore correct properly the experimentally determined number of atoms per row, since in the measurements only the mean entrance or detection direction is fully aligned with a crystallographic axis.

VI. RESULTS AND DISCUSSION

A. Standard single-alignment experiments

Surface-peak integrals have been measured for various beam energies between 500 and 1800 keV for an incident

^{4}He beam parallel to the [100] axis, perpendicular to the terraces. The detection could not be performed at grazing emergence, since the movable detector was equipped with a small aperture, and blocking effects (mainly planar) could hardly be avoided. The detection was achieved hence at $\theta_{lab}=165°$, with a great solid angle, on the fixed detector. For this reason we were limited by background subtraction problems at low beam energies, and experiments below 500 keV would not have been sufficiently precise. The background subtraction was performed using the procedure tested in Ref. 22, i.e., drawing a straight line between the minimum level behind the surface peak and zero at the channel corresponding to the peak maximum. Typical [100] single-alignment spectra recorded with 0.5- and 1.8-MeV ^{4}He are represented in Figs. 11(a) and 11(b). At 1.8 MeV, the shape of the surface peak is due to the two copper isotopes ^{65}Cu and ^{63}Cu. The surface-peak integrals were calibrated using the Ta standards and taking into account deviations from the Rutherford cross section given in Ref. 23, which are significant for high-Z target atoms at low energies (for instance, a 12% correction is needed between Cu and Ta at 200 keV, and a 4% correction is needed at 500 keV). We have estimated our overall uncertainty for the number of atoms per row associated with the surface peak to be of the order of $\pm 7\%$ (taking into account background subtraction, standard precision, and statistics).

The results are presented in Fig. 12 as a function of the parameter ρ_B/R, where ρ_B corresponds to the bulk-atom vibrations. They are compared to two simulations for a perfect crystal. In the first, the surface vibrations ρ_S are assumed equal to ρ_B. In the second case we took $\rho_S=1.5\rho_B$. The two calculations do not lead to very different results, demonstrating that the experiments are not very sensitive to surface vibration amplitude; they are both in agreement with the measurements within the experimental uncertainties. Therefore, the results appear very similar to results on channeling studies reported in the literature for surfaces which are considered as well ordered. However, the following remarks are necessary. (i) As indicated in Sec. V, correlated vibrations are not taken into account in the calculations and an additional discrepancy of $\simeq 15\%$ cannot be excluded; (ii) one atom per row corresponds to two atomic layers, and a 7% discrepancy at the limit of our experimental uncertainty corresponds consequently to $\simeq 30\%$ of an atomic layer at 500 keV and $\simeq 60\%$ at 1800 keV. These experiments are therefore not very precise for studying the structure of the first surface plane.

However more valuable information should be obtained about surface structure from single-alignment experiments by optimizing the choice of the axial direction studied, the detection angle, and the incident-beam energy. For instance, along the [101] axis one atom per row corresponds to one (100) atomic plane. The surface peak along this direction, using 200-keV ^{4}He beams, is expected to be of the order of 1.7 atoms/per row and hence is indicative of displacements in or from the first atomic plane. Such experiments require detection in a grazing emergence geometry in order to lower the bulk background. As already stated, such a detection could not be achieved in our setup in single-alignment geometry. However, as will be seen in the next section, the same type of information was extracted from double-alignment experiments.

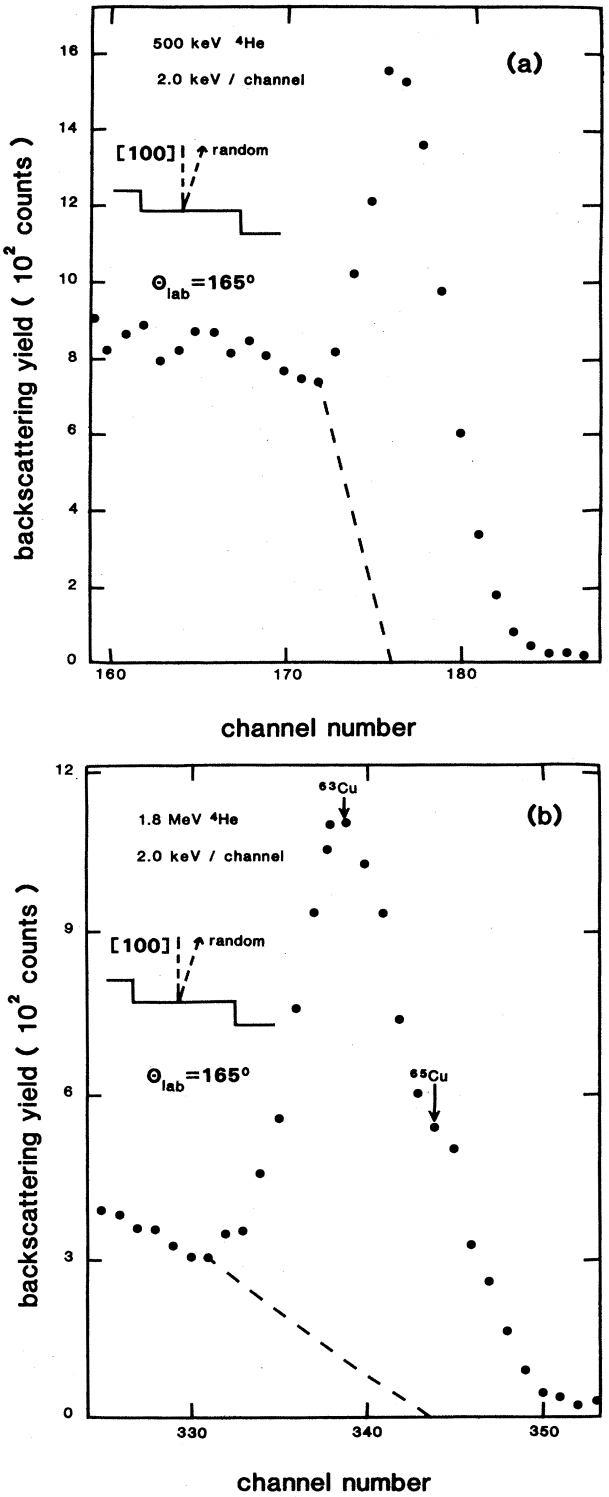

FIG. 11. Typical single-aligned spectra at (a) 500 keV and (b) 1800 keV. The background subtraction procedure is shown. Care must be taken at 1800 keV for the subtraction of the contribution by the two Cu isotopes.

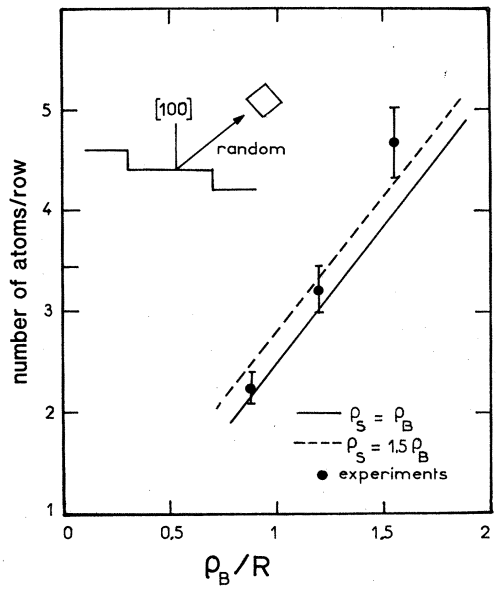

FIG. 12. Number of atoms per row in [100] single-alignment experiments with various beam energies, as a function of ρ_B/R. The experimental points are compared to values computed by Monte Carlo simulations for two values of the surface vibration ρ_S.

B. Search for surface relaxation

1. *Clean surfaces*

A typical double-aligned spectrum, with the beam entering along the [100] axis as in Sec. VI A but with detection along the [101] axis at 45°, is presented in Fig. 13. The beam energy is 200 keV, and the crystal temperature is 300 K. The peak-to-background contrast is very good and no problems arise in background subtraction. The surface-peak integral corresponds to 1.7 (100) atomic plane with an uncertainty, which is in this case estimated to be smaller than 4%. The surface peak for a perfect crystal with identical surface and bulk vibrations can be calculated to correspond to 1.5 (100) atomic plane. The comparison of the experimental and calculated values indicates that the surface plane is mostly ordered, even though the small discrepancy observed might support the presence of some disorder. Note that for this experiment the calculated value is somewhat overestimated, on the one hand, because correlated vibrations are neglected, but underestimated on the other, since enhanced surface vibrations perpendicular to the sample surface should affect the blocking of the beam detected at 45°. These two effects are likely to compensate each other roughly, and the calculated value seems realistic.

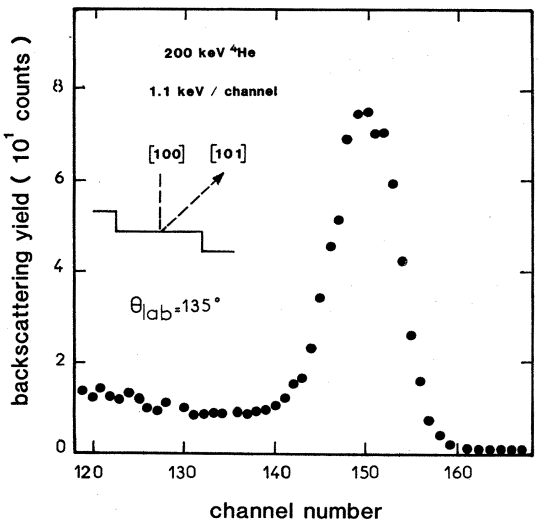

FIG. 13. Experimental spectrum in [100]→[101] double-alignment geometry. The surface peak corresponds to 1.7 atom/[101]. Note the very low background.

An angular scan across the [101] axis is presented in Fig. 14. In this experiment, the detector is moved in the (010) plane perpendicular to the terraces. The angular scan corresponding to an energy window behind the surface peak is also represented in the figure and allows a precise determination of the [010] axis position. The surface dip appears as slightly asymmetrical and shifted, indicating a surface relaxation leading to a displacement of 0.035 Å perpendicular to the [101] axis. This displacement, which is at the sensitivity limit of our measurements, corresponds to a surface contraction of 0.05 Å. Our result can be written as a contraction of 0.05±0.05 Å, i.e., 3±3% of the (100) interplanar spacing (1.8 Å). This is in agreement with the very low relaxations calculated in Ref. 11 and estimated by LEED measurements in Ref. 12 for instance, for Cu(100).

It is of interest to note that the low-energy ion scattering measurements of Ref. 16 on (410) stepped Cu structures also indicate only a very small contraction of the order of 2%. Our experiments therefore provide for the second time evidence that the surface relaxation of (100)

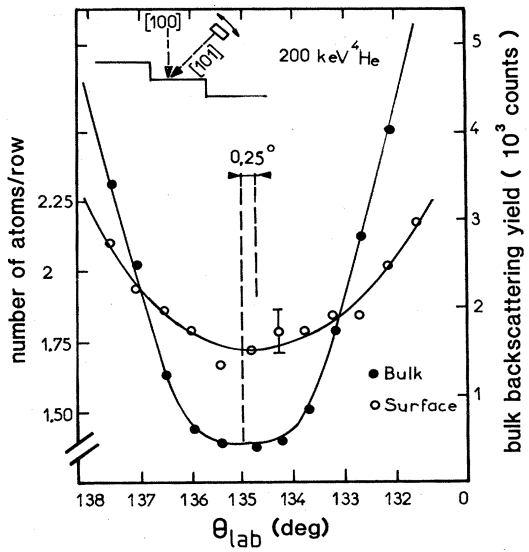

FIG. 14. Surface and bulk blocking dips across the [101] axis in the [100]→[101] double-alignment geometry. The comparison of the two dips (slight shift and asymmetry of the surface dip), indicates a small contraction of the first interplanar spacing.

terraces in stepped Cu structures is very similar to that of flat (100) surfaces.

2. *Effect of oxygen adsorption*

The same experiments were repeated after oxygen adsorption at saturation coverage ($N_O = 7.6 \times 10^{14}$ cm^{-2}), i.e., on a mixed (100) and (410) surface (see Sec. III C).

The surface-peak integral (200-keV incident ^{4}He), for detection in the [101] direction corresponds now to 2.0 (100) atomic planes, i.e., a significant enhancement with respect to "clean" surfaces. This can be either due to a much stronger relaxation or to surface disordering (see Sec. IV B 3). The first hypothesis was checked by recording angular scans across the [101] as done previously. The surface scan presented in Fig. 15 shows the same degree of asymmetry and shift as that of Fig. 14, but in the opposite direction. We can therefore conclude a surface expansion of $3 \pm 3\%$ of a (100) interspacing. The change from surface contraction to surface expansion when oxygen is adsorbed is in agreement with the channeling observations of Ref. 15 for Ni. Since the absolute value of the relaxation is of the same order of magnitude for clean or oxygen-covered surfaces, the discrepancy between the surface-peak integrals at the minimum of the scans for these two situations cannot be attributed to relaxation effects. A surface disordering related to oxygen adsorption must be considered therefore.

In the experimental angular scans represented in Figs. 14 and 15, the contrast between minimum and maximum is, as indicated in Sec. IV A, rather low ($\simeq 25\%$). The scatter between the experimental surface-peak integrals at a given angular position (mainly statistics on the countings) never exceeded 4—5 % (i.e. 0.1 atom per row), but this is already significant owing to the low overall contrast. For this very reason we have considered that our uncertainty in the relaxation measurement was rather high and the relaxations observed were at the limit of this sensitivity. However, the trend observed in Figs. 14 and 15 were always confirmed by repeating the experiments. The solid lines drawn through the experimental points were obtained by a least-square-fit procedure.

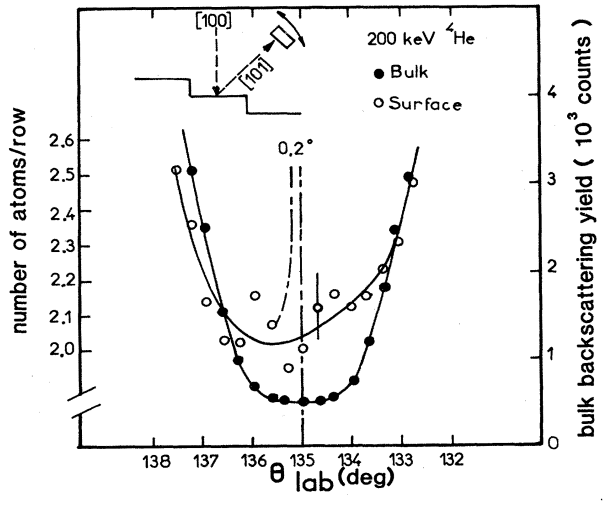

FIG. 15. Same scans as in Fig. 13, but on the sample with oxygen adsorbed at saturation coverage. The comparison of the surface and bulk scans now indicates a small surface expansion.

C. Study of the surface plane: 90° double alignment experiments

A preliminary remark must be made about data reduction. The surface peaks correspond to a given number of atoms per cm^2, i.e., to a given fraction of the first atomic plane. In order to convert this result to atoms/row and allow the comparison with calculations, the mean number of atoms per row in the terraces, N_T, must be known with good precision. This means that the angle between the macroscopic surface and the (100) terraces must be measured accurately. For this purpose, we first aligned the movable detector with the (011) axis of the terraces perpendicular to the step edges and then measured what angle this detector had to be rotated in order to obtain a total extinction of the counting rate. The uncertainty in such a measurement is related to both the solid angle of detection and to multiple-scattering events in the surface region. The angle measured in this way was $5 \pm 0.2°$. We therefore have a 4% uncertainty on N_T. The other uncertainties are related to the precision on the backscattering standards, the subtraction of the background (which is usually very low), and the statistics. In this type of experiment, the latter uncertainty is often significant. The overall uncertainty on the number of atoms per row determined in the 90° double-alignment experiments has been estimated to be $\pm 10\%$.

1. *Study of the step-edge relaxation*

As indicated in Sec. IV B 1, these studies require blocking experiments along the two major axes of the terraces [011] and [001] which all contain a step-edge atom.

A typical double-aligned [100]→[011] spectrum, obtained with 200-keV ^{4}He ions on the crystal at 300 K, is shown in Fig. 16. The surface peak superimposed on a very low bulk background contribution corresponds to

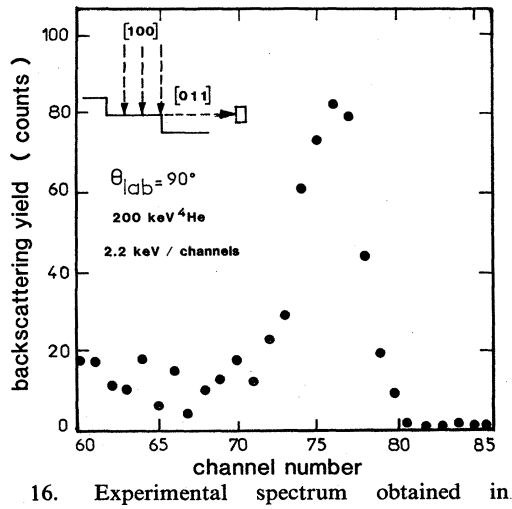

FIG. 16. Experimental spectrum obtained in the [100]→[011] geometry (90° double alignment). The surface peak corresponds to 0.3 (100) atomic plane and is displayed with almost no background.

4.5×10^{14} atoms/cm^2, i.e., to 0.3 atomic plane. Such a spectrum is recorded in a few minutes, with rather high beam currents of the order of 50 nA. The beam dose is about 10 μC. In Fig. 17, the spectrum of Fig. 16 is compared to a spectrum recorded in identical conditions but for the position of the detector, which is moved from $\theta_{lab}=90°$ to 92.2° or symmetrically to 87.8°. In the latter situation, the backscattered particles penetrate into the crystal and emerge at the first step edge they meet. Since this situation does not correspond to a perfect double alignment, the yield, and particularly the surface-peak yield, increases markedly. This result proves that surface roughness is very low: Note also that there is no significant broadening of the surface peak. The minimum observed at 90° is hence indeed due to blocking and not to geometrical screening effects. It is of interest to notice that in the experiments presented here, the depth resolution is around 20 Å, set by the 10-keV energy resolution of the detector. With an electrostatic analyzer of the type used in Ref. 24, and even replacing ^{4}He ions by protons, the nominal resolution would be of the order of one interplanar spacing (1.8 Å).

The experimental angular scans presented in Fig. 18 represent the surface and the bulk yields near the [011] blocking axis. ^{4}He beams of 200 keV were sent on the sample at 300 K. The minimum surface yield measured in this experiment corresponds to 2.5 atoms/row. The surface dip is symmetrical and centered at an angle corresponding to the bulk minimum yield. This implies that the relaxation of the edge atoms perpendicular to the terraces is smaller than 0.05 Å or 3% of (100) interspacing (see Secs. IV B 1 and V).

Preliminary studies of a possible edge-atom relaxation in the (100) terrace plane, perpendicular to the step edges, made by measuring an angular scan around the [001] blocking axis (see Sec. IV B 1), were also undertaken. The

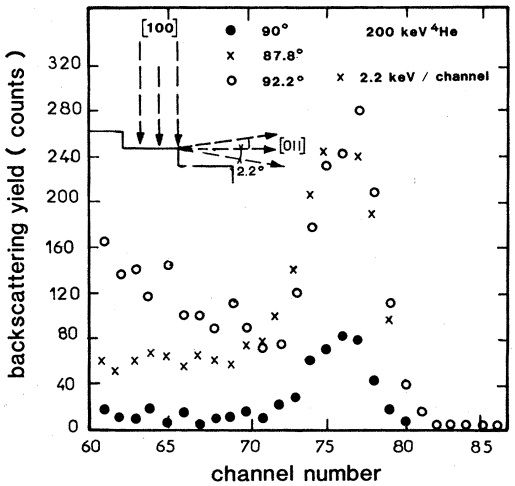

FIG. 17. Experimental spectra obtained in, or near, the [100]→[011] geometry. The two surface peaks recorded with the detector ±2.2° off the [011] axis are identical in width and integral, indicating surface roughness is very low and does not affect the experiments. Note the lower background at $\theta_{lab}=87.8°$ in comparison with that at $\theta_{lab}=92.2°$, associated with the more grazing emergence.

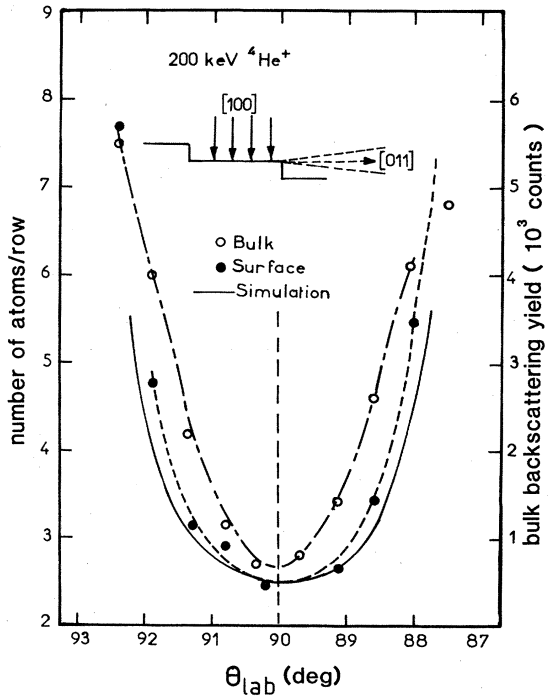

FIG. 18. Surface and bulk blocking scans across the [011] axis near the 90° double-alignment geometry. The symmetry and minimum position of the surface dip indicates essentially no specific vertical relaxation of the edge atoms. The simulated surface dip also displayed, calculated with $\rho_S=1.5\ \rho_B$, fits the bottom of the experimental scan, but is slightly wider (see text).

results do not indicate a significant relaxation. A more detailed study on this point is in progress.

Our results are in contradiction with those of Ref. 16 in which a 10% contraction of the interplanar spacing has been indicated near the step edges for Cu(410) structures. We do not believe that this contradiction is only due to the fact that the (100) terraces are wider in the (16,1,1) than in the (410) structure. In the result of Ref. 16 (measurements by low-energy ion scattering) the authors find at the same time that the mean interplanar distance between two terraces is nearly conserved. This means that the terraces are highly distorted, owing to their small width and to the strong edge effect. Such a distortion could not remain unseen in our experiments. A possible explanation for the absence of edge relaxation in our case could be related to surface contamination. We have reported in Sec. III B that the amount of C and O atoms trapped at the surface was, respectively, about 5% and 3% of a Cu(100) atomic plane. On the other hand, the edge atoms represent, for the (16,1,1) structure, about 12% of the surface atoms. Since they are likely to be highly reactive and to constitute preferential adsorption sites, it is very possible that they have trapped most of the light impurities, and this environment could prevent relaxation. This hypothesis is supported by the fact that we have recently performed preliminary experiments on (410) Cu structures which indicate significant step-edge relaxation, in agreement with Ref. 16.

Another important feature indicated by our results is that, although small, the minimum surface yield measured

along the [011] and [001] blocking directions is significantly higher than the calculated yield assuming a perfect crystal and surface thermal vibrations identical to those of the bulk. The measured values are, respectively, 2.5 and 2.2 atoms/row for [011] and [001], and the calculations give 1.7 and 1.45 atoms/row. In both cases the ratio between experimental and calculated values is 1.5, i.e., much higher than the maximum ratio of 1.1 which would be consistent with our experimental uncertainties. Such a description of the surface is hence not correct. However, since the difference between experimental and calculated values is smaller than 1 atom/row, the edge atoms cannot be considered to be in a fully random position. Three possible explanations may be given for the observed discrepancies.

(i) The edge atoms are highly disordered. This is not inconsistent with the absence of relaxation of these atoms: The relaxation corresponds to a coherent displacement of the edge and cannot be assimilated to disorder.

(ii) The whole surface plane is somewhat disordered.

(iii) The surface thermal vibrations are significantly higher than in the bulk, and the step-edge atom vibrations are even higher than those of atoms inside the terraces.

Of course, all three explanations could be partly true. In order to discriminate between all these possibilities, we have performed experiments by varying the beam energy, the sample temperature, and the studied axial direction in the terraces.

2. *Study of the terrace structure*

A simple way to test whether the edge atoms play a major role in the discrepancies observed is to study given blocking directions and to vary the contribution of these atoms to the surface peak by varying the beam energy.

Measurements were therefore performed at 500 keV along the [001] direction and 500 and 1000 keV along the [011] direction. In the latter case, for example the number of atoms per row measured is equal to 5.7, i.e., to 0.7 atomic plane and the step-edge contribution is only 17%. However, for all the experiments performed in this way, the ratio between experimental results and calculations for a perfect "bulklike" surface remains constant and equal to 1.5. This result demonstrates that the edge atoms are, in terms of disorder and vibration, in the same situation as the other terrace atoms.

A tempting explanation in terms of enhanced surface-thermal vibrations of all the surface atoms could be given for the constancy of the ratio. However, owing to the high value of this ratio and the fact that only the component of the vibration normal to the surface is expected to vary significantly, such an explanation would imply that this component $\langle u_z^2 \rangle^{1/2}$ of the vibration is extremely high. In particular, our result would predict a somewhat lower surface Debye temperature Θ_{DS_z} for Cu than calculated in Ref. 17. The surface yield is nearly proportional to ρ, the rms value of the vibration perpendicularly to the axis studied. Our measurements, interpreted exclusively in terms of enhanced vibrations, therefore imply that, e.g., if the thermal vibration in the terrace plane is assumed nearly equal to the bulk vibration, the component normal to the surface is $\simeq 1.8$ times higher than in the bulk.

In order to check this possibility we have studied, for the [011] and [001] blocking directions, the influence of temperature on the surface-peak integral: Further experiments were performed at 600 K. The bulk Debye temperature for Cu is around 315 K. Assuming surface vibrations to be responsible for the results obtained at 300 K, the "surface Debye temperature" Θ_{DS_z} should be around 170 K. Assuming this value to hold, the surface vibrations ρ_S at 600 K can be calculated. The temperature dependence of ρ_S between 300 and 600 K is nearly like $\sqrt{T}$ with only a 3% correction due to deviations from a harmonic model.[25] Since in the same domain the bulk vibrations ρ_B also vary nearly like $\sqrt{T}$, the ratio between experimental and calculated surface-peak integrals (which is equal to ρ_S/ρ_B) should be temperature independent. This is not the case: We observe that this ratio increases markedly at 600 K and reaches values around 2 instead of 1.5 at 300 K for experiments performed with 200- and 500-keV beams. This result demonstrates that surface disordering occurs when the sample is heated, and consequently that some disorder could already be present at 300 K and could (at least partly) account for the observed discrepancies.

The nature of this disorder is such that it produces very similar effects to those due to thermal vibrations on the surface-peak areas (see, for example the constancy of the discrepancy as a function of beam energy and for the two directions studied at 300 K), but it has a different temperature dependence. Thermal vibrations imply that a given atom has a probability distribution around its mean postion, while the disorder considered here implies that each atom has a mean position (i.e., averaged over themal vibrations) such that the distribution of these mean positions, with respect to regular lattice sites, for all surface atoms is similar in shape and of the same order of magnitude in spatial extension as the thermal-vibration distribution for a single atom. Such defects, which from our experimental results appear to be quasi-isotropically distributed, can be accounted for in Monte Carlo simulations simply by broadening the atom distribution, i.e., by introducing a fitting value ρ_{app} higher than the thermal vibrations ρ_B in the bulk. Of course, ρ_{app} is both related to defects and thermal vibrations and does not follow the temperature dependence characteristic of real thermal vibrations.

We must point out that, even by using the value ρ_{app} fitting the experimental value of the surface peak for aligned spectra, some discrepancy remains between experiment and simulation when studying the angular dependence of the surface peak. A calculated angular scan obtained with $\rho=\rho_{\text{app}}$ is compared in Fig. 18 to the experimental blocking dip for the [100]→[011] situation. The calculated scan is about 10% wider. This disagreement may be due to the fact that the correlations in atomic displacements are neglected in our simulations. If they were taken into account, higher values of ρ_{app} would be needed in order to fit the experimental values at the bottom of the scans. In such a situation the calculated dip would likely be somewhat narrower and a better overall fit would be observed.

As a matter of fact, we have some experimental evidence for the important role played by the correlations in

atomic displacements. This role is demonstrated when studying the more minor [012] axis along the terraces (see Sec. IV B 2).

We find that along [012] the ratio between experimental surface-peak integrals and calculations for bulklike perfect surfaces is equal to 2 for experiments performed with 200- and 500-keV ions with the sample at 300 K. This ratio is markedly higher than in the case of [001] and [011] directions at the same temperature. This result shows again that disorder is not larger for step-edge atoms, which are not present in most of the [012] axes, than for other surface atoms. It moreover indicates that the correlation in atomic displacements (static and dynamic) of near-neighbor atoms is strong and tends to lower the surface-peak yields measured for low-index axes. A more realistic value of ρ_{app} is hence expected to be obtained from experiments along the [012] direction.

The number of atoms per row measured in the various experiments described above are plotted in Fig. 19 as a function of ρ_B/R, along with the Monte Carlo calculated curves corresponding to the ratios ρ_{app}/ρ_B leading to the best fit. The ratio ρ_{app}/ρ_B corresponding to the [012] direction, which is expected to give the best information about the rms displacement, is equal to 2. In this case, $\rho_{app}=0.17$ Å at 300 K. It appears difficult to evaluate for

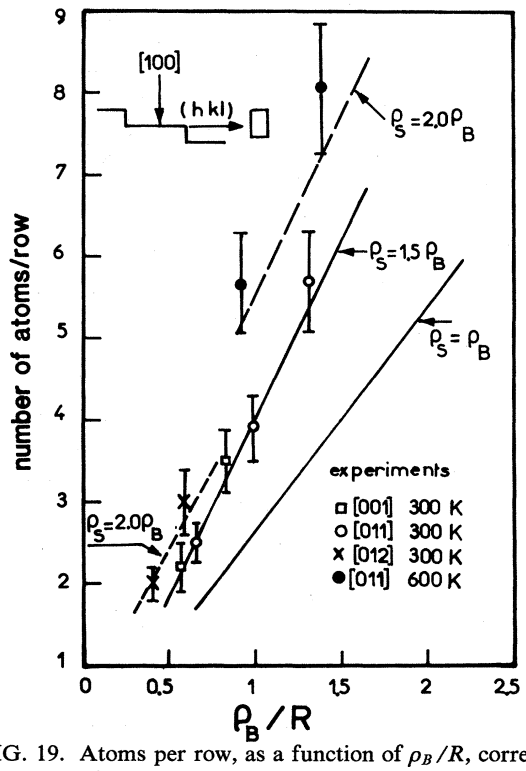

FIG. 19. Atoms per row, as a function of ρ_B/R, corresponding to the surface peak in 90° double-alignment experiments for various axes in the terraces. The experiments were also performed at various beam energies, and sometimes at two temperatures (300 and 600 K). The curves displayed were obtained by Monte Carlo simulations for various surface vibrations ρ_S. The two dashed lines were calculated for $\rho_S=2\rho_B$, assuming either that only the first three atoms of the row vibrate with ρ_S (case of [210]) or that ρ_S is associated with the first eight atoms (case of [011] or [001]).

this value the relative contributions of thermal vibrations and static displacements. If the thermal-vibrations rms is taken as equal to ρ_B, the rms static displacement would be of about 0.14 Å. However, due to enhanced surface thermal vibrations, the true value of the static displacements is probably smaller, of the order of 0.10 Å at 300 K.

The surface defects indicated in our experiments may be due to various causes: interactions with impurities, adatoms, or advacancies, step-edge interactions, etc. They may possibly be due to the stepped structure; however, since they can only be measured in 90° double-alignment experiments, the standard channeling experiments not being sufficiently sensitive, and since in our case the latter experiments lead to results similar to those obtained on many unstepped flat surfaces, they may possibly also be present in these cases.

Recent results on various Cu surfaces studied by very-low-energy (≃50 meV) He diffraction reported by Lapujoulade *et al.* in Ref. 25 for stepped surfaces are of great help in order to check this last possibility. These authors find that for the flat closed-packed surfaces such as (111) or (100) their data are consistent with the concept of a well-ordered surface, with surface vibrations in good agreement with those calculated in Ref. 17 in a very wide temperature domain (between 70 and 770 K). On the contrary, strong deviations from this picture are observed around a transition temperature between 300 and 500 K owing to the surface, when less dense (110) or stepped (113), (115), and (117) orientations are studied. This is interpreted by the authors of Ref. 25 as a roughening transition associated with the formation of structural defects such as adatoms, advacancies, kinks, etc. The results of Ref. 25 for stepped surfaces are very close to our observations and, in particular, with the disorder increase observed in our case between 300 and 600 K. Following the conclusions of Ref. 25, the temperature at which this disorder is created should depend strongly on the surface orientation and would be lower for stepped structures.

3. *Influence of oxygen coverage on surface disorder*

A [100]→[011] double-aligned spectrum has been taken, after oxygen adsorption at saturation coverage, with 200-keV ^{4}He, the sample being at 300 K. As indicated in Sec. IV B 3, the faceting observed is not expected to modify the surface-peak integral, unless this process is associated with disorder enhancement. This is indeed the case, since the surface-peak integral corresponds in this experiment to 4 atoms/row instead of 2.5 measured on the clean crystal. Oxygen adsorption is hence shown to induce strong surface disordering. Note that this conclusion has already been drawn, in a less definite way, from the results obtained in Sec. IV B 2 in the case of [100]→[101] double alignment at 45°.

VII. SUMMARY AND PERSPECTIVES

We have demonstrated that channeling in the 90° double-alignment geometry is a highly sensitive technique for studying stepped surface structures. In addition to information specific to these structures, such experiments may provide more general information about surface dis-

order, which are difficult to obtain by other ways. The present work was devoted to the study of vicinal copper surfaces structured in regular (100) terraces with kinkless steps. We have measured the saturation oxygen coverage for these structures, this coverage leading, as previously seen, to faceting.[2] The surface relaxation has been measured for clean and oxygen-covered surfaces. A small surface contraction ($\simeq 3\%$) in the first case and an expansion of the same order in the second case have been found. The result for the clean surface is in agreement with calculations[11] and LEED measurements.[12] The inversion of relaxation under oxygen is similar to previous results on Ni surfaces from other authors.[15] The very small relaxations measured in our case are at the limit of precision of our method.

The structure of the first atomic plane has been studied. No step-edge relaxation could be found either perpendicular to the terraces, or in the terrace plane perpendicular to the edges. Surface disorder that consists of small ($\simeq 0.1$ Å at 300 K) quasi-isotropic displacements with respect to regular sites are observed. These displacements are strongly correlated and temperature dependent, supporting recent results reported in Ref. 25. The step atoms are not significantly more displaced than the other surface atoms. Oxygen coverage increases surface disorder.

We think that similar studies should be performed in the near future. They would provide valuable information on surface structure and vibrations.

Some problems arise when regarding the present results. First of all, the surface cleanliness should be improved. In particular, impurity trapping at the step edges may have taken place and could affect step-atom relaxation and vibrations. Moreover, as demonstrated by the faceting under oxygen, the (16,1,1) surface is highly unstable under impurity adsorption. This might well be responsible (but only partly so) for the defects observed. In addition to surface cleanliness improvement, the study of more stable vicinal Cu surfaces would hence be of interest. This is the case, for example, for the (410) surface which remains stable under oxygen. The study of such a surface should also provide information about the possible influence of step-edge—step-edge interactions on surface disordering, since the step width is half as small as in the (16,1,1) case. Such studies would also allow one to check the surface-orientation dependence of the roughness transition temperature indicated in Ref. 25. Finally, in order to obtain valuable results on surface thermal vibrations, their influence on surface-peak integrals should be distinguished from that of static defects. This requires a systematic study of the temperature behavior of the surface peak down to low temperatures. It has been seen in particular that static defects increase strongly when the sample is heated. They may therefore become negligible at low temperature (the recent results of Ref. 25 also support this hypothesis), allowing a detailed study of the amplitude and correlations of surface thermal vibrations.

ACKNOWLEDGMENTS

This work was supported by the Central National de la Recherche Scientifique (CNRS), under Cooperative Research Program (RCP) No. 157. The authors are indebted to E. D'Artemare for improvements of the beam handling system of the 2-MV Van de Graaff accelerator which allowed us to couple the ultrahigh-vacuum chamber and to use stable, well-collimated beams at low energies. G. Amsel has demonstrated a constant interest in the work since its beginning. His major contribution to the design of the ultrahigh vacuum system, his discussions about the experiments and their interpretation, and, finally, his criticisms on the manuscript were most useful and are gratefully acknowledged.

*Permanent address: Dipartimento di Fisica G. Galilei, Università degli Studi di Padova, Via Marsolo 8, I-35100 Padova, Italy.

[1]H. Wagner, in *Solid Surface Physics,* Vol. 85 of *Springer Tracts in Modern Physics,* edited by G. Höhler (Springer, Berlin, 1979), p. 151.

[2]J. C. Boulliard, J. L. Domange, and M. Sotto (unpublished).

[3]S. Rigo, C. Cohen, A. L'Hoir, and E. Backelandt, Nucl. Instrum. Methods **149**, 721 (1978).

[4]G. Amsel, J. P. Nadai, C. Ortega, S. Rigo, and J. Siejka, Nucl. Instrum. Methods **149**, 705 (1978).

[5]M. Vidal, thesis, Conservatoire National des Arts et Métiers (Paris), 1972 (unpublished).

[6]M. Henzler, Surf. Sci. **19**, 159 (1970).

[7]C. Argile and G. E. Rhead, Surf. Sci. **53**, 659 (1975).

[8]J. C. Boulliard (unpublished).

[9]P. Wynblatt and N. A. Gjostein, Surf. Sci. **22**, 125 (1970).

[10]R. P. Gupta, Phys. Rev. B **23**, 6265 (1981).

[11]V. Landman, R. N. Hill, and M. Mostaller, Phys. Rev. B **21**, 448 (1980).

[12]G. M. E. Laramore, Phys. Rev. B **9**, 1204 (1974).

[13]D. L. Adams, H. B. Nielsen, J. N. Andersen, I. Stensgaard, R. Feidenhans'l, and J. E. Sorensen, Phys. Rev. Lett. **49**, 669 (1982).

[14]W. C. Turkenburg, R. G. Smeenk, and F. W. Saris, Surf. Sci. **74**, 181 (1978).

[15]J. F. Van der Veen, R. G. Smeenk, R. M. Tromp, and F. W. Saris, Surf. Sci. **79**, 212 (1979).

[16]A. J. Algra, S. B. Luitjens, E. P. Th. M. Suurmeijer, and A. L. Boers, Appl. Surf. Sci. **10**, 273 (1982).

[17]G. Armand, J. Lapujoulade, and Y. Lejay, in *Proceedings of the Seventh International Vacuum Congress and Third International Conference on Solid Surfaces, Vienna, 1977,* edited by R. Dobrozemsky *et al.* (R. Dobrozemsky, Vienna, 1978), p. 1361.

[18]J. H. Barrett and D. P. Jackson, Nucl. Instrum. Meth. **170**, 115 (1980).

[19]R. S. Nelson, M. W. Thomson, and M. Montgomery, Philos. Mag. **1**, 1385 (1962).

[20]J. Lindhard, Mat. Fys. Medd. Dan. Vid. Selsk. **35**, 1 (1965).

[21]G. Moliere; Z. Naturforsch. **2A**, **133** (1947).

[22]I. Stensgaard, L. C. Feldman, and P. J. Silverman, Surf. Sci. **77**, 513, (1978).

[23]J. L'Ecuyer, J. A. Davies, and N. Matsunami, Nucl. Instrum. Methods **160**, 337 (1979).

[24]W. C. Turkenburg, W. Sozka, F. W. Saris, H. H. Kersten, and B. C. Golenbrander, Nucl. Instrum. Methods **132**, 587 (1976).

[25]J. Lapujoulade, J. Perreau, and A. Kara, Surf. Sci. **129**, 59, (1983).

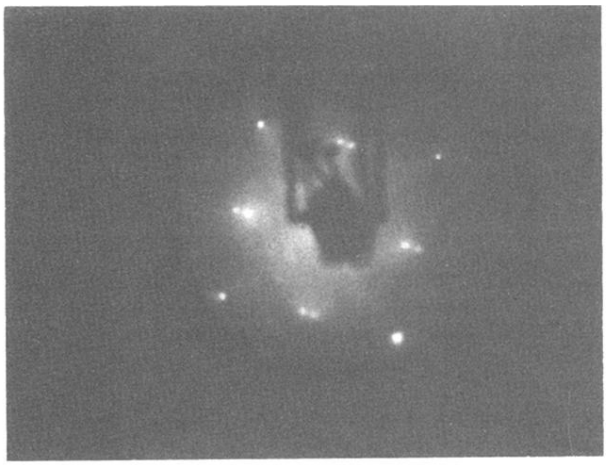

FIG. 3. LEED pattern on a clean (16,1,1) Cu surface. The double spots are characteristic of the stepped structure. Electron-beam energy: 123 eV.

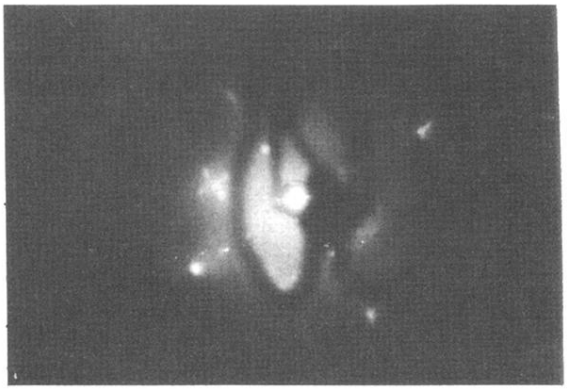

FIG. 4. LEED pattern on the sample after oxygen adsorption at saturation coverage. This diagram is characteristic of faceting in (100), (410), and (401) domains. Electron-beam energy: 114 eV.